

Assessment of the stress-strain state of machine structural elements made of polymer composite materials with a hybrid matrix by numerical simulation

E. Kosenko^{1*}, V. Nelyub², and V. Zorin¹

¹Moscow Automobile and Road Construction State Technical University (MADI), 64, Leningradsky Prospekt, 125319 Moscow, Russian Federation

²Bauman Moscow State Technical University, 2nd Baumanskaya, 105005 Moscow, Russian Federation

Abstract. The expansion of the fields of application of polymer composite materials (PCM) requires the development of their new compositions, structures, and molding methods. One of the most difficult tasks in the design of PCM products is the selection or development of a polymer matrix that meets a number of technological and operational requirements. The addition of components forming an independent conditionally liquid phase to the composition of the PCM matrix makes it possible to change the set of properties of the composite and ensure its high crack resistance. The paper presents the results of evaluating the stress-strain state of model samples of carbon fiber reinforced plastic with an organosilicon polymer material that forms a hybrid matrix with the base material of the binder. Modeling was carried out for cases of using organosilicon material with low and high modulus of elasticity. Also, modeling of a front-end loader bucket made using carbon fiber with the considered hybrid matrix was performed. The simulation results showed that the use of PCM with organosilicon material in the manufacture of a product can significantly reduce its weight and provide a sufficient margin of safety.

1 Introduction

The production of structural elements of machines from metals and their alloys is characterized by a high labor intensity of the technological process. In addition, providing the necessary margin of safety for such products leads to their high metal consumption and, accordingly, a large mass of products, which, in turn, negatively affects the fuel efficiency and environmental friendliness of the operation of such equipment. Among the known methods for reducing the mass of products while ensuring their operational properties, the most widely used is the replacement of metal structural materials with polymer composite materials.

* Corresponding author: KosenkoKate@mail.ru

Composite materials have high values of specific strength and rigidity, fatigue life, can be operated in a wide temperature range, have a low temperature coefficient of linear expansion, and also have a relatively low density, which greatly expands the technological possibilities of their application [1–4] and, therefore, the use of composite materials. materials becomes one of the most important factors determining the competitiveness of manufactured products [5-8].

At present, polymer composite materials (PCM) are most widely used on the international and Russian markets. When creating these materials, one of the most important tasks is the choice or development of a polymer matrix (binder) that will ensure maximum strength characteristics and will satisfy operational and technological requirements [9, 10].

Depending on the specific destruction mechanism, the matrix material and adhesive interactions that occur at the “reinforcing material – binder” interface affect the limiting characteristics of products in different ways, which complicates the process of choosing or developing optimal matrices. The variety of PCM failure mechanisms is also associated with the problems of calculating and predicting its characteristics [11].

In addition, for the most accurate idea of the characteristics of a product created using PCM, it is necessary to comprehensively study its physical and mechanical properties and behavior in various climatic conditions [12–14].

The conducted studies have shown that the addition of an organosilicon polymer material to the composition of the PCM matrix, which forms an independent phase in the composite structure and represents a hybrid matrix together with the base material, makes it possible to minimize the loss of mechanical properties of the product during the transition to the region of extremely low temperatures (at $t = -30^{\circ}\text{C}$). C and -50°C). At the same time, the creation of a soft intermediate layer (made of an organosilicon polymer material) makes it possible to reduce the excessive rigidity of the product structure, which in some cases is important when increasing its durability [15].

Figure 1 shows the organosilicon polymer material in the PCM structure is a uniform boundary layer of reduced strength. Figure 1b shows this component of the hybrid matrix forms one transition layer with the binder material, bounded on both sides. The formation of such a transition layer is determined by the colloid-chemical mechanism.

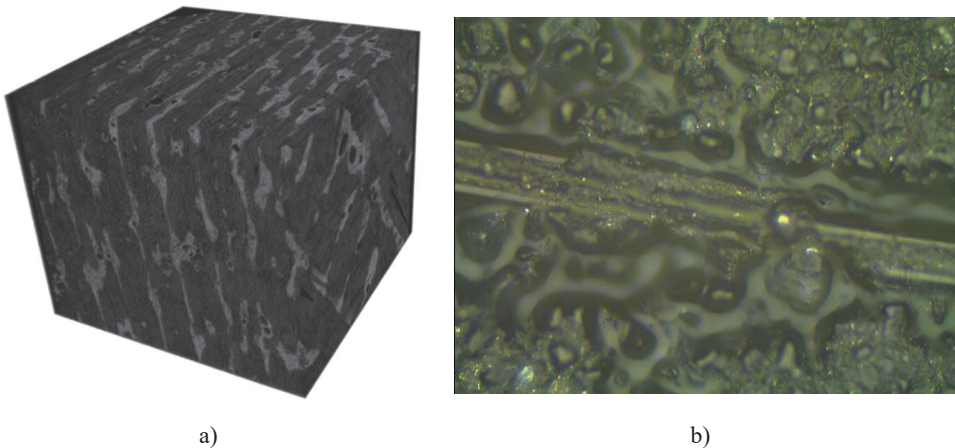


Fig. 1. The results of the evaluation of the structure of PCM with an organosilicon polymer material, obtained using an X-ray microtomograph of the SkyScan 1172 brand (a) and an optical microscope at a magnification of $\times 1000$ (b).

A weak interface at fracture makes it possible to relieve increased stresses near the crack, which makes the composite non-brittle and practically insensitive to cracks across the fibers [16–18].

The assessment of the stress-strain state (SSS) of PCM with an organosilicon polymer material in the matrix structure is an important scientific and practical problem, the solution of which will make it possible to predict the behavior of engineering products made from such a composite under various operating modes and operating conditions.

The purpose of this work is to study the mechanism of failure of PCM with an organosilicon polymer material in the composition of a hybrid matrix and to evaluate the possibility of slowing down or stopping the growth of cracks by an interface formed by an organosilicon material.

2 The stress-strain state of model samples of polymer composite materials with a hybrid matrix assessment

As an object in assessing the stress-strain state of PCM with a hybrid matrix, carbon fiber was taken, consisting of a fabric based on carbon fiber grade T-300 and an epoxy binder based on epoxy resin and an anhydride-type hardener. An organosilicon polymer material was used to form the boundary layer.

The initial data of carbon fiber (CFRP) used in the calculations are given in Table 1.

Table 1. Properties of carbon fiber based epoxy matrix.

Indicators	Characteristics along the axes		
	X	Y	Z
Modulus of elasticity, MPa	121000	8600	8600
	Characteristics in planes		
	XY	YZ	XZ
Poisson's ratio	0,27	0,4	0,27
Shear modulus, MPa	4700	3100	4700

The initial data of the matrices are presented in Table 2.

Table 2. Properties of materials used as matrices.

Indicators	Matrix	
	Epoxy	Organosilicon
Density, kg/m ³	1100	1060
Modulus of elasticity, MPa	3800	1 – 100
Shear modulus, MPa	1400	0.38 – 33.8
Poisson's ratio	0.35	0.48

Based on the results of structural analysis (see Fig. 1a), a computational model of a composite material with a hybrid matrix was developed (Fig. 2-4).

Depending on the complexity of the solid geometry, the finite element mesh is constructed from 10-node SOLID187 3D tetrahedral elements or SOLID186 20-node hexagonal elements. Contact pairs are created using flat surface-to-surface contact elements of the CONTA174 type. The grid contains 338371 nodes and 184287 elements.

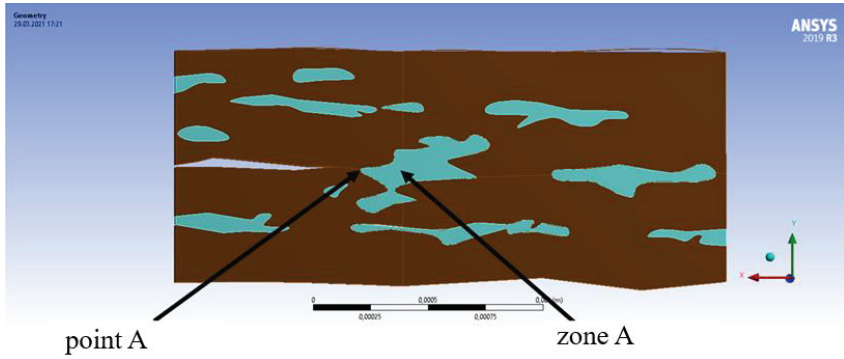


Fig. 2. Geometric model of a composite material.

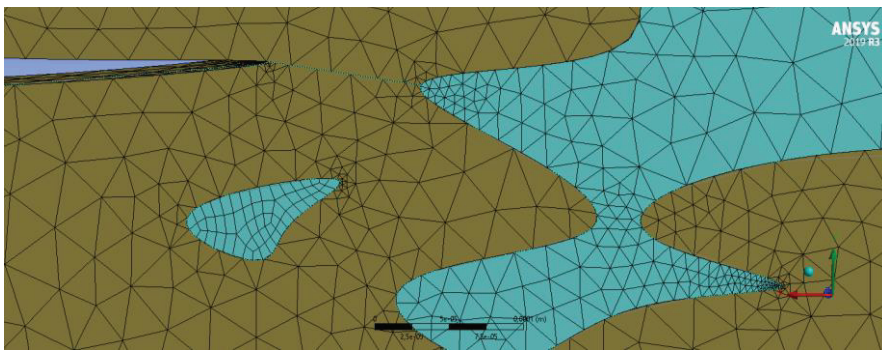


Fig. 3. Fragment of the model showing the dimensions of the finite elements.

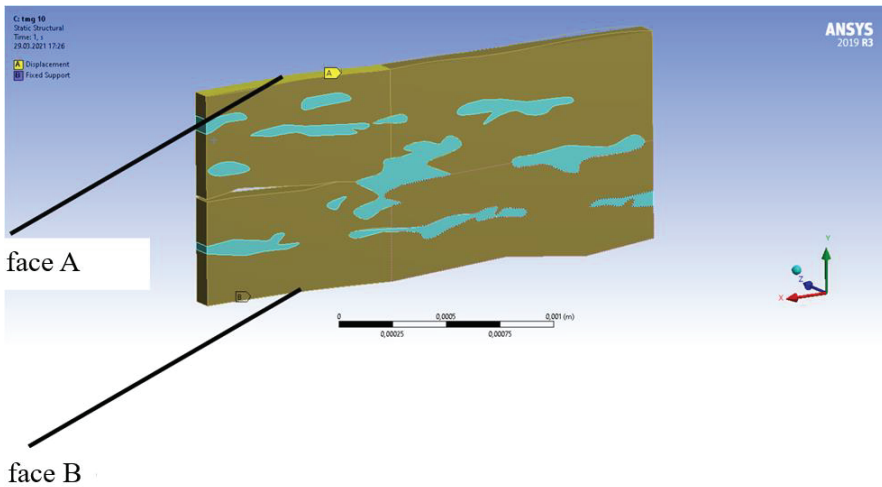


Fig. 4. Boundary conditions.

On figures 2-4 show in brown (dark) CFRP, consisting of only unidirectional carbon tapes and epoxy binder. Figure 4 shows the boundary conditions, face B is closed and face A is moved up. These boundary conditions make it possible to estimate the values of stresses during the occurrence of a crack and its subsequent growth.

Figure 2 shows the assessment of the stress-strain state was carried out at point A, Figure 2 also shows crack propagation or its stop is assumed in zone A.

On fig. Arrows in Figure 2 indicate point A, at which the stress-strain state was assessed. The same figure shows zone A, in which the crack will grow or stop, depending on the values of the maximum stresses at the crack tip and the ultimate stresses of the material in this zone.

Within the framework of the study, three design cases were considered in Table 3. The density of the composite material is assumed to be 1490 kg/m³.

Table 3. Compositions of composite materials used in VAT calculations.

Sample №	Phase composition. h			Modulus of elasticity of the organosilicon matrix. MPa
	Fiber	Epoxy matrix	Organosilicon matrix	
1	0.52	0.33	0.15	10
2		0.33	0.15	500
3		0.48	–	–

Samples No. 1 and No. 2 are a composite material with hybrid matrices, one of which is epoxy, and the second is elastomeric. In this case, in sample No. 1, the elastomer is in a conditionally liquid state, and in sample No. 2, the elastomer is in a cured state. Sample No. 3 is a carbon fiber reinforced plastic with a high content of the epoxy matrix. In this sample, the epoxy matrix occupies the entire volume, which in samples No. 1 and No. 2 was occupied by the hybrid matrix (epoxy + elastomeric).

The calculations used the initial data of carbon fiber, given in table. 1. Composite material has such characteristics, which in fig. 2-4 is shown in brown.

Figure 5 shows the maximum displacements for all four (Table 2) considered design cases are close to each other, while Figures 6-7 show the maximum stress values differ significantly from each other.

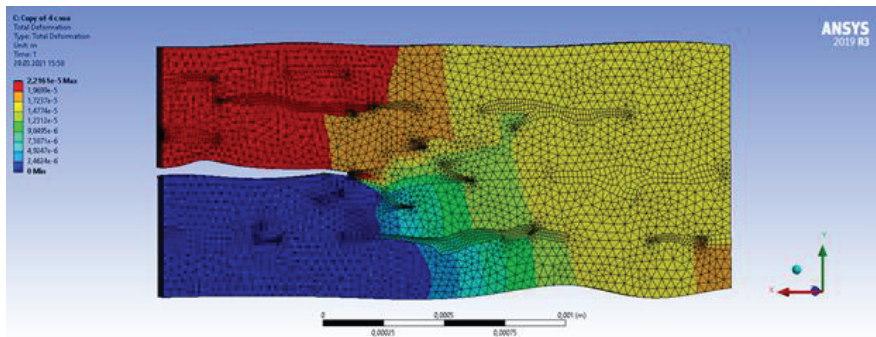


Fig. 5. Displacement calculation results.

For convenience of analysis, the results obtained are given in Table. 4.

Table 4. Results of the assessment of the stress-strain state.

Design case. according to the table. 2	Material strength limit. MPa	Design stress at the crack tip. MPa	Margin of safety	The nature of the development of damage
1	40	33.4	1.2	Crack growth stopped
2	50	144.7	0.35	Slow crack growth
3	55	1410	0.04	Fast crack growth

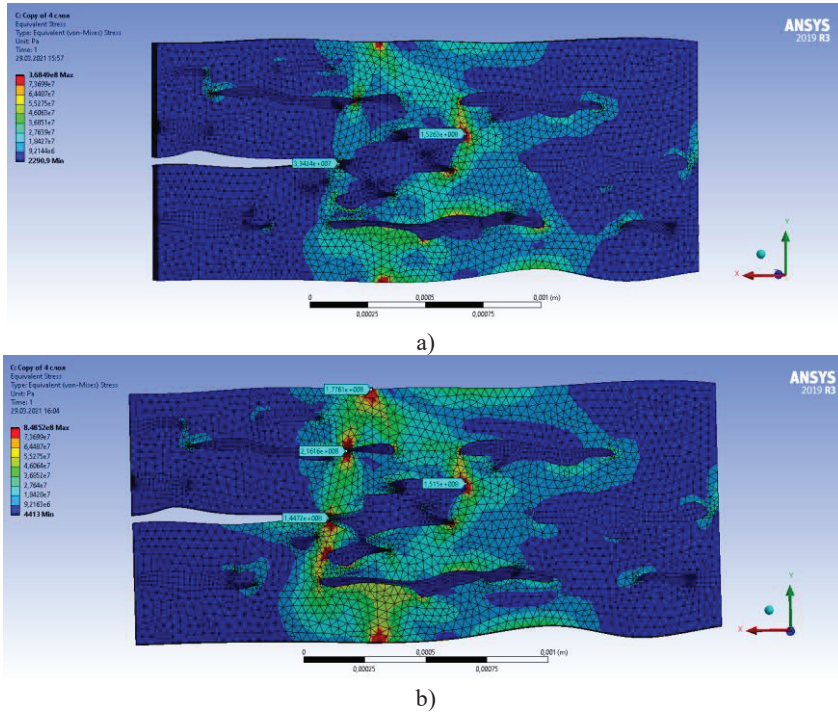


Fig. 6. The results of calculating the maximum stresses in the composite material (a) No. 1, see Table. 2 (b), No. 2, see table. 3.

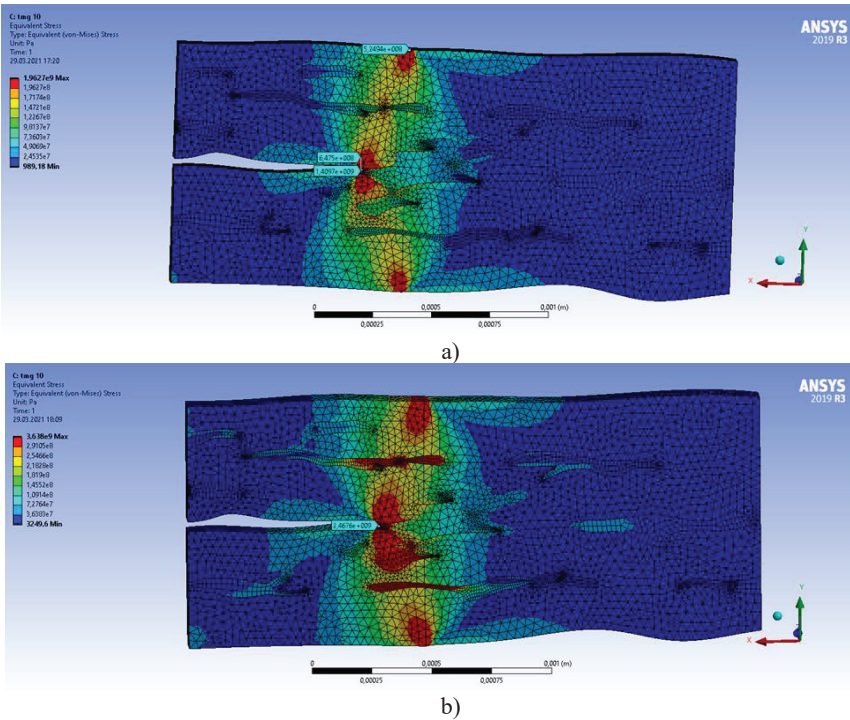


Fig. 7. Results of calculating the maximum stresses in composite material No. 3 (see Table 3) in the area where the epoxy matrix is located (a) and around it (b).

Analysis of the obtained results allows us to draw the following conclusions:

- CFRP has the highest margin of safety, which contains a “liquid” matrix with the lowest modulus of elasticity (No. 1);
- a significantly lower margin of safety has carbon fiber, in which an elastomer is used as a "liquid" matrix;
- the worst results were obtained for the composite, which contains an excess amount of epoxy matrix (No. 3).

In table. 3 shows the calculated values of stresses for all considered cases, but only for one point A, fig. 2 - stress values obtained under the condition that the crack propagates directly along zone A. It is this design case that led to such unexpected results in which sample No. 3, in which this zone is an epoxy matrix, has such a low safety margin.

On figures 6, 7 and in table. Figure 3 shows the results of a linear static strength calculation and determines the values of ultimate stresses without taking into account plasticity and imitation of the nature of fracture. A standard approach is used, in which, if the ultimate stress is less than the ultimate strength, then we assume that the crack growth stops. If the calculated stresses exceed the ultimate strength, then we assume that the crack continues to grow. Thus, only for sample No. 1, the limiting stresses do not exceed the allowable values either in the material of the matrix “liquid” phase component or in the composite, and it can be argued that this material acts as a crack energy damper.

3 Stress-strain state of machine structural elements on the example of a front loader bucket assessment

As a base product for an example of calculating the stress-strain state of machine structural elements made of polymer composite materials with a hybrid matrix, we will take the front bucket of a front-end loader, the volume of which is 2 m³, weight m=540 kg, width 2250 mm. Traditionally, the loader bucket is made of 09G2S steel sheets (density $\rho=7850$ kg/m³, elastic modulus $E=210$ GPa, yield strength $\sigma_T=320$ MPa, tensile strength $\sigma=480$ MPa) and Figure 8 shows a welded structure.

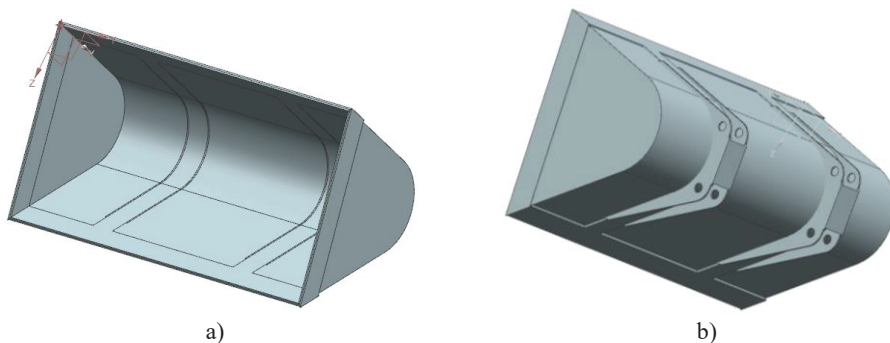


Fig. 8. Bucket design diagram: front view (a) and rear view (b).

A three-dimensional geometric model of the structure (shell and solid) was created in SiemensNX CAD (Fig. 9). For the convenience of analyzing the results obtained, the product was divided into two zones with single and double thickness. As can be seen from these figures, the product can be divided into zones with single and double thickness. When creating a finite element model in Ansys, this was done using the Shell Thickness tool.

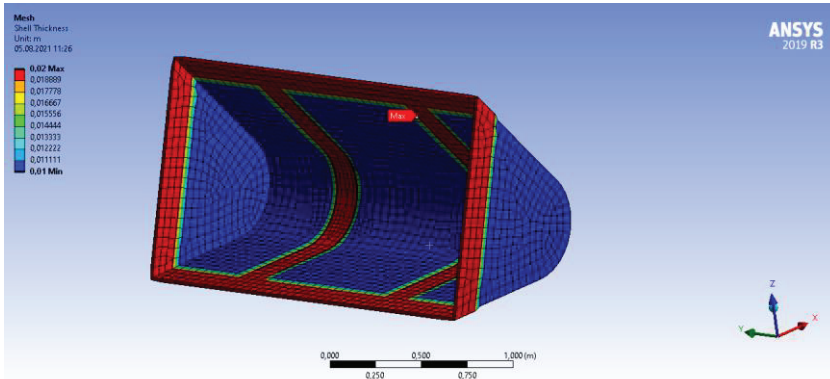


Fig. 9. Finite element model of a steel bucket of a front loader.

Consider the design case, when the loader moves forward in the process of clearing a snow-covered section of the road. Figure 10 shows as design loads, the own weight of the structure and a pressure of 15 kPa, uniformly applied over the inner surface of the ladle, were taken.

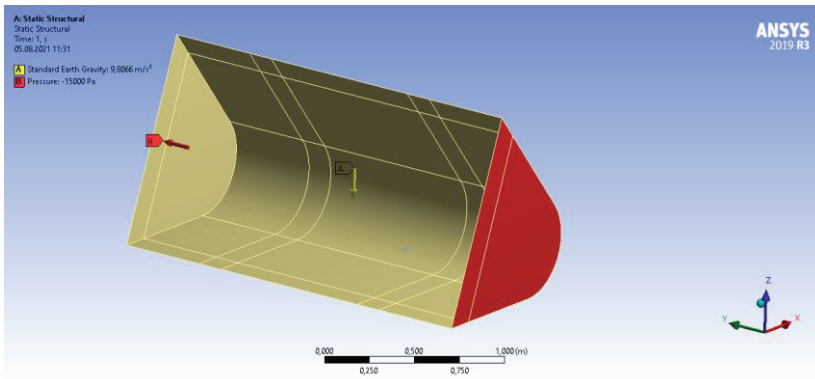


Fig. 10. Structure diagram showing load application points.

Figure 1 shows the fastening of the bucket on the loader arm is modeled using rotational articulated pairs (joint type Revolute).

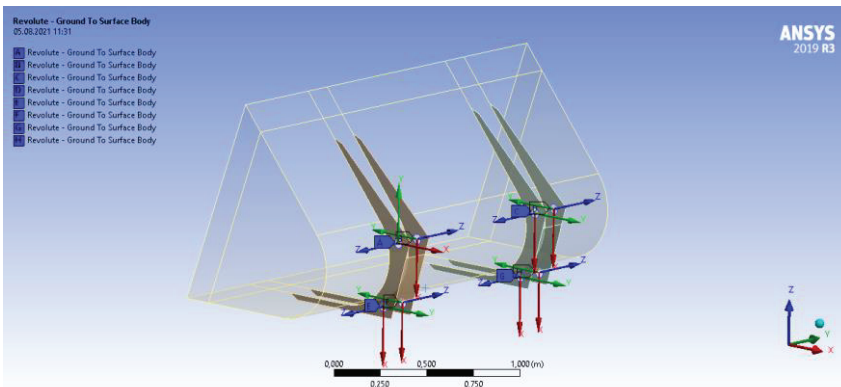


Fig. 11. Scheme of the construction of a metal bucket with an indication of the fixing points.

Figures 12 (a, b) show the results of stress and displacement calculations.

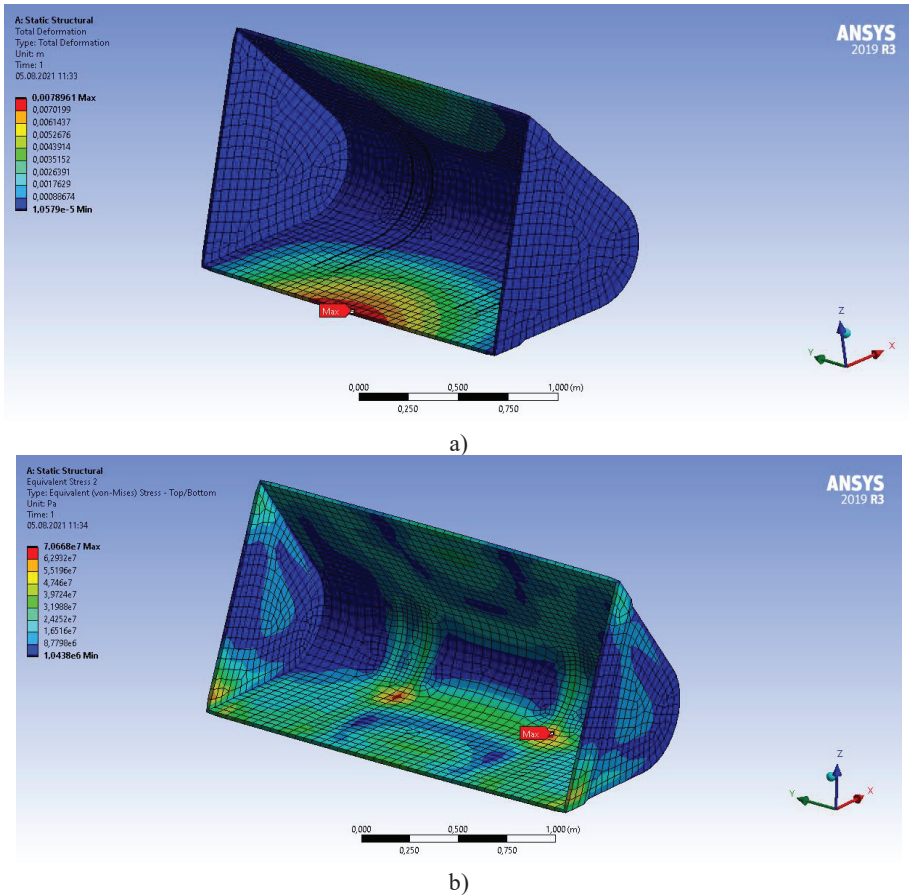


Fig. 12. The results of the calculation of displacements (a) and stresses (b) for the metal structure of the ladle.

As a result of the calculations, it was found that the safety margin for steel is about 4–5, while the product has a high mass, which leads to a decrease in productivity, fuel efficiency and environmental friendliness of the operation of the technical system as a whole.

Figure 12 shows the study of the stress field also allows us to conclude that the lower plane of the ladle is the most loaded in the corners of the structure and the butt zones, there are also increased stresses. As the practice of operating such products shows, it is these zones that are the places of formation of fatigue cracks that occur primarily in defects and zones of weakening of the metal around welds.

The use of polymer composite materials in the production of a loader bucket can significantly reduce its weight, reduce energy consumption and the load on the drive. In addition, the production of products from PCM makes it possible to implement their more complex forms, which, in turn, contributes to the expansion of functionality and performance. So, for example, changing the shape of the front loader bucket will avoid sticking of compacted materials, including snow mass in its corners.

Figure 13 shows a view of a loader bucket made using PCM with organosilicon material as part of a hybrid matrix with increased crack resistance.

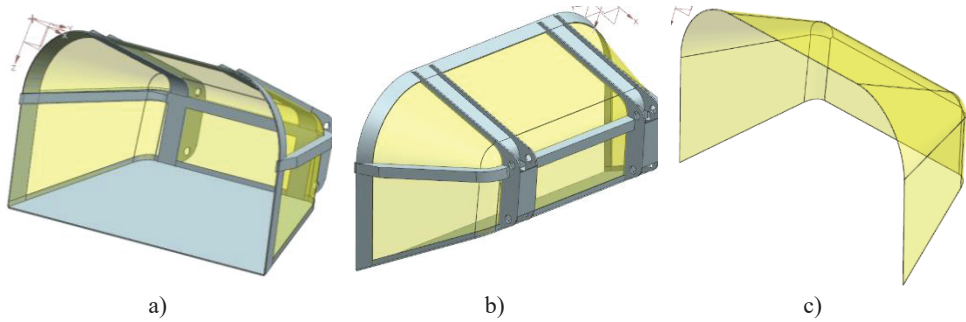


Fig. 13. Scheme of the design of the bucket with carbon fiber inserts: front view (a), rear (b) and side (c).

For the calculation, the data indicated in tables 5 and 6 were used.

Table 5. Characteristics of a composite material with a crack resistance of 500 J/m².

Indicators	Characteristics along the axes		
	X	Y	Z
Modulus of elasticity, MPa	121000	8600	8600
Tensile strength, MPa	2231	29	29
Ultimate compressive strength, MPa	1082	100	100
	Characteristics in planes		
	XY	YZ	XZ
Poisson's ratio	0,27	0,4	0,27
Shear modulus, MPa	4700	3100	4700
Shear strength, MPa	60	32	60

Table 6. Characteristics of a composite material with a crack resistance of 670 J/m².

Indicators	Characteristics along the axes		
	X	Y	Z
Modulus of elasticity, MPa	111320	8170	8170
Tensile strength, MPa	2050	27	27
Ultimate compressive strength, MPa	1015	95	95
	Characteristics in planes		
	XY	YZ	XZ
Poisson's ratio	0,29	0,41	0,29
Shear modulus, MPa	4324	2945	4324
Shear strength, MPa	65	36	65

Figure 13 shows the part of the bucket made of carbon fiber is a monolithic product of complex shape. To ensure the bearing capacity, including when the loader collides with solid objects, the lower surface of the bucket and the mounting area are made of sheet steel. The most loaded bucket zones are also reinforced with metal structures. The connection of the composite material and metal is carried out by glue mechanically. Composite material properties are set in the AnsysCompositePrepPost (ACP) module. Figure 14 shows the initial geometry in the form of a shell model was created in SiemensNX. The thickness distribution in the finite element mesh.

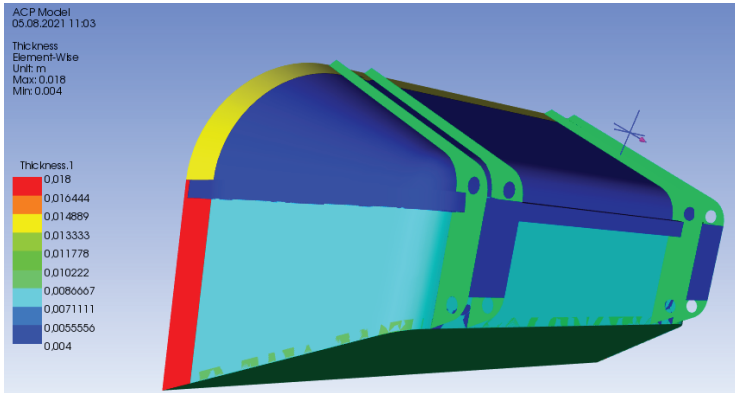


Fig. 14. Finite element model of a bucket made using carbon fiber.

The design of the ladle is designed in such a way that the thickness of the composite part of the product is much lower than in the original metal product. The laying is quasi-isotropic, from a set of tissue monolayers with an orientation of $0/90^\circ$ and $\pm 45^\circ$. At the same time, the mass of the structure is about 275 kg, of which only 30 kg fall on the share of carbon fiber. Similarly, to the calculation of the metal analogue considered above, the structure is loaded by gravity and a uniformly applied pressure of 15 kPa (Fig. 15). Figures 16, 17 and table 7 show the results of the VAT calculation.

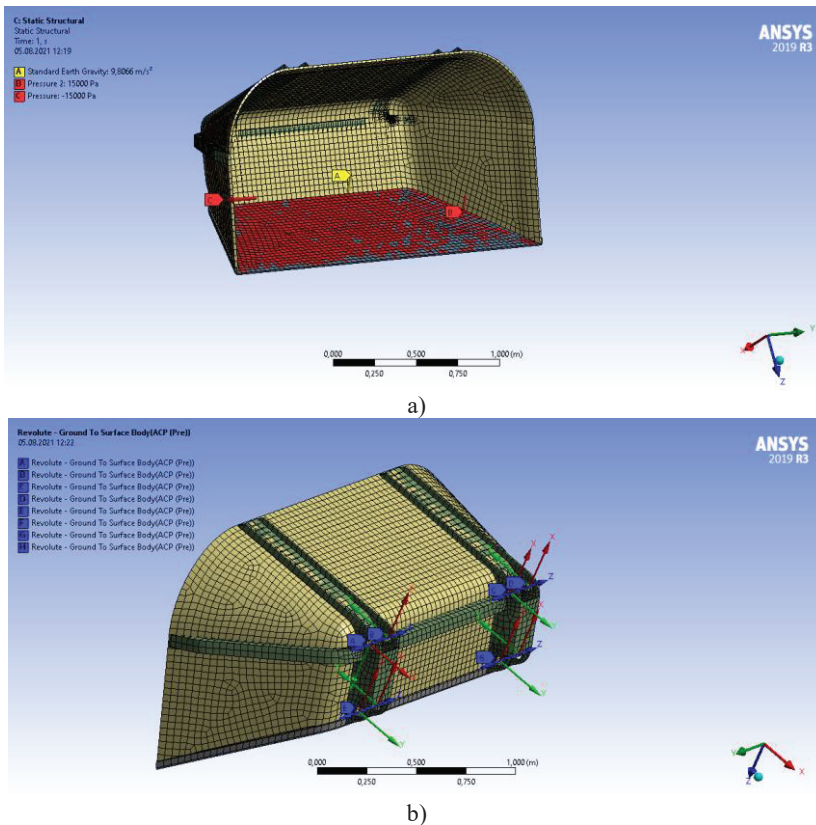


Fig. 15. Scheme of applying the load (a) and fixing (b) for the design of the bucket with parts made of carbon fiber.

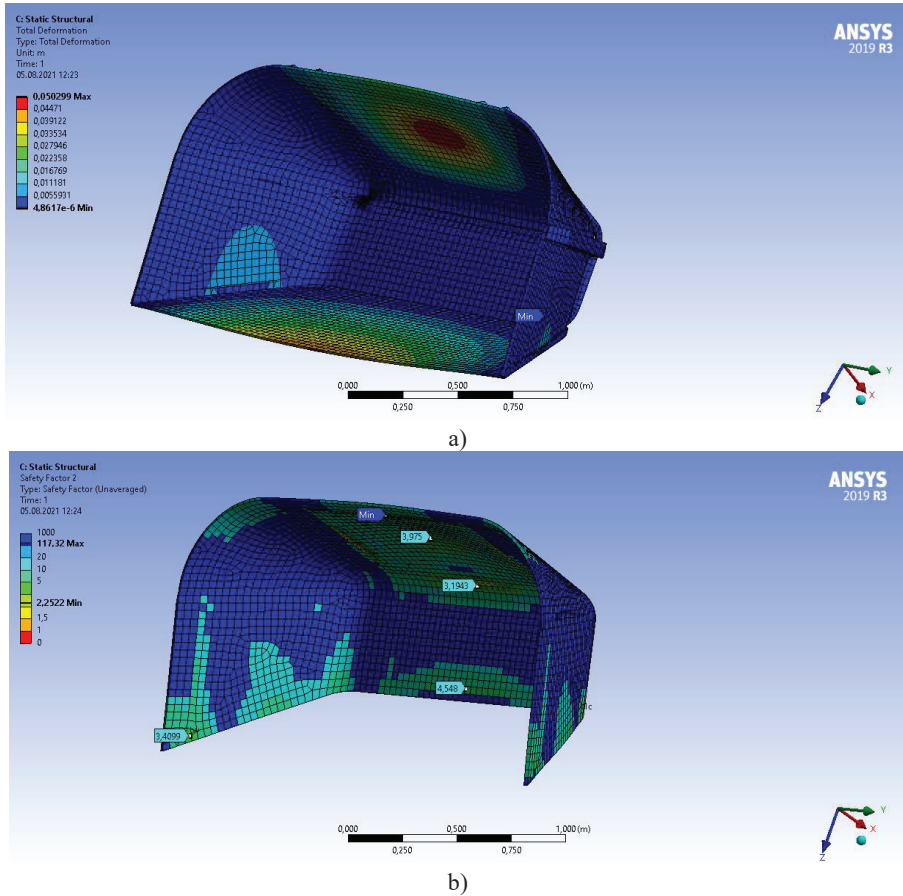


Fig. 16. The results of the calculation of displacements (a) and stresses (b) for the design of a bucket made of carbon fiber.

Table 7. The results of the calculation of the design of the bucket, made of various materials.

Indicators	Material		
	Steel 09G2S	CFRP with epoxy binder	CFRP on an epoxy binder with an organosilicon component
Margin of safety	4,5	2,1	2,25
Peak displacement, m	0,008	0,047	0,05
Product weight, kg	540	280	275

To assess the strength of a composite structure, the CompositeFailureTool built into AnsysMechanical was used, which makes it possible to determine the safety margin for various sets of failure criteria. In this case, the Cai-Wu and Pak criteria are used. As a result of the calculations, Figure 16 shows that the displacement field shows higher maximum values compared to the metal structure (see Fig. 12). Figure 16 (b) shows the distribution of safety factors in the design.

The minimum safety factor is 2.1, the average safety factor exceeds 3 times. For CFRP with a hybrid matrix, which does not tend to accumulate defects quickly, this corresponds to the level of long-term strength.

4 Conclusion

Thus, the simulation results showed that the presence of an organosilicon polymer material in the composition of the PCM matrix in a liquid or highly elastic state leads to a significant change in the crack growth rate.

If the organosilicon polymer material in the composition of the PCM matrix is in an uncured (liquid) state, that is, it has the lowest modulus of elasticity, stress relaxation takes place in such a composite and the crack stops growing, since the limiting stresses do not exceed the allowable values either in the organosilicon itself matrix material, nor in the composite.

If the organosilicon material in the composition of the hybrid PCM matrix is in a hardened state, i.e., it has a high modulus of elasticity, then the interface formed by it makes it possible to slow down the growth of a crack.

The lowest safety factor and the highest crack growth rate are typical for the sample, in the composition of the matrix of which there was no organosilicon matrix.

Acknowledgments

The material was prepared as part of scientific research under project No. FSFM-2020-0011 (2019-1342), experimental studies were carried out using the equipment of the CKP MADI

References

1. V.A. Nelyub, B.L. Gorberg, M.V. Grishin et al, *Fibre Chemistry* **50(6)**, 524-527 (2019)
2. A.S. Borodulin, V. Nelyub, A.K. Shaov et al, *International Journal of Pharmaceutical Research* **12(3)**, 2323-2328 (2020)
3. E.O. Platonova, E. Vlasov, V.A. Nelyub, A.V. Polezhaev, *Journal of Applied Polymer Science* **136(33)**, 47869 (2019)
4. P.P. Maung, T.L. Htet, G.V. Malysheva, *IOP Conference Series: Materials Science and Engineering* **709(2)**, 022041 (2020)
5. L.P. Kobets, A.S. Borodulin, G.V. Malysheva, *Fibre Chemistry* **48(4)**, 311-315 (2016)
6. A.S. Borodulin, A. Kalinnikov, A. Kharaev, S. Shcherbin, *IOP Conference Series: Materials Science and Engineering* **302(1)**, 012062 (2019)
7. A.S. Borodulin, A.N. Kalinnikov, *SIOP Conference Series: Materials Science and Engineering* **709(2)**, 022038 (2020)
8. P.A. Belov, A.S. Borodulin, L.P. Kobets, G.V. Malysheva, *Polymer Science-Series D* **9(2)**, 205-208 (2016)
9. C. Yanyan, V.A. Nelyub, G.V. Malysheva, *Polymer Science-Series D* **12(3)**, 296-299 (2019)
10. A.N. Marycheva, T.A. Guzeva, P.M. Pe et al, *Polymer Science-Series D* **12(2)**, 170-173 (2019)
11. I.V. Bessonov, M.N. Kopitsyna, A.V. Polezhaev, V.A. Nelyub, *Polymer Science-Series D* **9(1)**, 17-21 (2016)
12. I.G. Marenkov, N.I. Baurova, *Journal of Physics: Conference Series* **1990(1)**, 012077 (2021)
13. I.G. Marenkov, N.I. Baurova, *Polymer Science - Series D* **14(4)**, 489–492 (2021)

14. M.D. Vasiliev, I.A. Komarov, *Journal of Physics: Conference Series* **1990(1)**, 012075 (2021)
15. E.A. Kosenko, V.A. Zorin, *Journal of Physics: Conference Series* **1990(1)**, 012070 (2021)
16. E.A. Kosenko, N.I. Baurova, V.A. Zorin, *Russian Metallurgy (Metally)* **2020(13)**, 1518–1521 (2020)
17. E.A. Kosenko, N.I. Baurova, V.A. Zorin, *Polymer Science - Series D* **13(3)**, 341–344 (2020)
18. J.E. Gordon, *The New Science of Strong Materials: Or Why You Don't Fall Through the Floor* (Princeton University Press, 2006)